ANTIMICROBIAL AGENTS AND CHEMOTHERAPY, Oct. 2011, p. 4560–4568 Vol. 55, No. 10
0066-4804/11/$12.00 doi:10.1128/AAC.00519-11

Antagonistic Interactions of *Pseudomonas aeruginosa* Antibiotic Resistance Mechanisms in Planktonic but Not Biofilm Growth▽

Xavier Mulet,[1]† Bartolomé Moyá,[1]† Carlos Juan,[1] María D. Macià,[1] José L. Pérez,[1] Jesús Blázquez,[2] and Antonio Oliver[1]*

Servicio de Microbiología and Unidad de Investigación, Instituto Universitario de Investigación en Ciencias de la Salud (IUNICS), Hospital Universitari Son Espases, Ctra. de Valldemossa 79, 07014 Palma de Mallorca, Spain,[1] and Centro Nacional de Biotecnología—Consejo Superior de Investigaciones Científicas (CSIC), C. Darwin 3, 28049 Madrid, Spain[2]

Received 17 April 2011/Returned for modification 27 May 2011/Accepted 22 July 2011

Pseudomonas aeruginosa **has an extraordinary capacity to evade the activity of antibiotics through a complex interplay of intrinsic and mutation-driven resistance pathways, which are, unfortunately, often additive or synergistic, leading to multidrug (or even pandrug) resistance. However, we show that one of these mechanisms, overexpression of the MexCD-OprJ efflux pump (driven by inactivation of its negative regulator NfxB), causes major changes in the cell envelope physiology, impairing the backbone of *P. aeruginosa* intrinsic resistance, including the major constitutive (MexAB-OprM) and inducible (MexXY-OprM) efflux pumps and the inducible AmpC β-lactamase. Moreover, it also impaired the most relevant mutation-driven β-lactam resistance mechanism (constitutive AmpC overexpression), through a dramatic decrease in periplasmic β-lactamase activity, apparently produced by an abnormal permeation of AmpC out of the cell. While these results could delineate future strategies for combating antibiotic resistance in cases of acute nosocomial infections, a major drawback for the potential exploitation of the described antagonistic interaction between resistance mechanisms came from the differential bacterial physiology characteristics of biofilm growth, a hallmark of chronic infections. Although the failure to concentrate AmpC activity in the periplasm dramatically limits the protection of the targets (penicillin-binding proteins [PBPs]) of β-lactams at the individual cell level, the expected outcome for cells growing as biofilm communities, which are surrounded by a thick extracellular matrix, was less obvious. Indeed, our results showed that AmpC produced by *nfxB* mutants is protective in biofilm growth, suggesting that the permeation of AmpC into the matrix protects biofilm communities against β-lactams.**

Pseudomonas aeruginosa is one of the most frequent and severe (up to 50% mortality) causes of acute nosocomial infections (31). No less concerning, chronic respiratory infection by *P. aeruginosa* is the main driver of morbidity and mortality in patients with cystic fibrosis and other chronic respiratory diseases (18).

The treatment of these infections is severely compromised by the extraordinary capacity of this pathogen to evade the activity of nearly all available antibiotics through a complex interplay of intrinsic and mutation-driven resistance pathways (4, 16). The biofilm mode of growth, a hallmark of chronic infections, provides *P. aeruginosa* populations with differentiated structural and physiological properties that further enhance its capacity to escape from the activity of antimicrobial treatments (3, 9). Among the most relevant resistance pathways, in both acute and chronic infections, are those leading to the overexpression of the chromosomal β-lactamase AmpC, which is frequently triggered by the inactivation of the nonessential penicillin-binding protein PBP4 and confers high-level resistance to antipseudomonal penicillins and cephalosporins (20), along with the inactivation of the carbapenem porin OprD or the overexpression of several efflux pumps encoded in its genome (16, 17, 25). Unfortunately, the combinations of these resistance pathways are often additive or synergistic, leading to multidrug (or even pandrug) resistance. However, one of these mechanisms, overexpression of the MexCD-OprJ efflux pump (caused by inactivation of its negative regulator NfxB), besides conferring resistance to the pump substrates, determines a marked hypersusceptibility to other relevant antipseudomonal agents, including most β-lactams and aminoglycosides (8), perhaps suggesting the occurrence of antagonistic interactions with other resistance mechanisms.

During the initial steps of this research, we learnt that it is in fact the case that overexpression of this efflux pump impairs highly relevant resistance mechanisms; the β-lactam resistance driven by the overexpression of AmpC is particularly worth noting. These results prompted us to follow a global approach to decipher the complexity of the underlying mechanisms, providing relevant information for the identification of new targets for fighting *P. aeruginosa* intrinsic and acquired resistance mechanisms, but with a major drawback resulting from the differential bacterial physiology characteristics of biofilm communities, a hallmark of chronic infections.

* Corresponding author. Mailing address: Servicio de Microbiología, Hospital Son Espases, Ctra. Valldemossa 79, 07010 Palma de Mallorca, Spain. Phone: 34 871 20 62 62. Fax: 34 871 90 97 08. E-mail: antonio.oliver@ssib.es.

† X.M. and B.M. contributed equally to the work.

▽ Published ahead of print on 1 August 2011.

MATERIALS AND METHODS

Strains, plasmids, and construction of PAO1 knockout mutants. The complete list of strains and plasmids used or constructed in this work is shown in Table 1. Single- and multiple-knockout *nfxB*, *mexD*, *dacB* (*PBP4*), *oprM*, *mexR*,

TABLE 1. Strains and plasmids used or constructed in this study

Strain or plasmid	Genotype and relevant characteristic(s)[a]	Reference or source
Strains		
P. aeruginosa		
PAO1	Reference strain completely sequenced	Laboratory collection
PAΔdacB	PAO1 Δ*dacB*::*lox dacB*, encoding the nonessential PBP4	20
PAΔC	PAO1 Δ*ampC*::*lox ampC*, encoding the chromosomal β-lactamase AmpC	21
PAONB	PAO1 Δ*nfxB*::*lox nfxB*, encoding the nefative regulator (NfxB) of MexCD-OprJ efflux pump	23
PAOMxD	PAO1 Δ*mexD*::*lox mexD*, encoding the MexD efflux pump component	23
PAOD1	Spontaneous *oprD* null mutant (W65X) of PAO1	22
PAOM	PAO1 Δ*oprM*::*lox oprM*, encoding the outer membrane protein component of MexAB-OprM and MexXY-OprM efflux pumps	This work
PAOMxR	PAO1 Δ*mexR*::*lox mexR*, encoding the negative regulator of MexAB-OprM efflux pump	This work
PANBdB	PAO1 Δ*nfxB*::*lox* Δ*dacB*::*lox*	This work
PANBMxD	PAO1 Δ*nfxB*::*lox* Δ*mexD*::*lox*	This work
PANBAC	PAO1 Δ*nfxB*::*lox* Δ*ampC*::*lox*	This work
PANBOM	PAO1 Δ*nfxB*::*lox* Δ*oprM*::*lox*	This work
PAdBOM	PAO1 Δ*dacB*::*lox* Δ*oprM*::*lox*	This work
PANBdBOM	PAO1 Δ*nfxB*::*lox* Δ*dacB*::*lox* Δ*oprM*::*lox*	This work
PANBdBMxD	PAO1 Δ*nfxB*::*lox* Δ*dacB*::*lox* Δ*mexD*::*lox*	This work
JW	Wild-type *P. aeruginosa* clinical isolate	35
JWNB	JW Δ*nfxB*::*lox*	This work
GPP	Wild-type *P. aeruginosa* clinical isolate	35
GPPNB	GPP Δ*nfxB*::*lox*	This work
E. coli		
XL-1 blue	F′::Tn10 *proA*$^+$*B*$^+$ *lac1*^{q}Δ(*lacZ*)M15 *recA1 endA1 gyrA96* (Nal^r) *thi hsdR17* (r_k^- m_k^-) *mcrB1*	Laboratory collection
S17.1	RecA pro (RP4-2Tet::Mu Kan::Tn7)	Laboratory collection
Plasmids		
pUCP24	Gm^r, pUC18-based *Escherichia-Pseudomonas* shuttle vector	32
pUCPNB	Gm^r, pUCP24 containing wild-type *nfxB* from PAO1	This work
pEX100Tlink	Ap^r, *sacB*, pUC19-based gene replacement vector with an MCS	26
pUCGm*lox*	Ap^r, Gm^r, pUC18-based vector containing the *lox* flanked *aacC1* gene	26
pCM157	Tc^r, *cre* expression vector	26
pEXdacBGm	pEX100Tlink containing 5′–3′ flanking sequence of *dacB*::Gm*lox*	20
pEXACGm	pEX100Tlink containing 5′–3′ flanking sequence of *ampC*::Gm*lox*	21
pEXNBGm	pEX100Tlink containing 5′–3′ flanking sequence of *nfxB*::Gm*lox*	23
pEXMxDGm	pEX100Tlink containing 5′–3′ flanking sequence of *mexD*::Gm*lox*	23
pEXMxR	pEX100Tlink containing 5′–3′ flanking sequence of *mexR*	This work
pEXMxRGm	pEX100Tlink containing 5′–3′ flanking sequence of *mexR*::Gm*lox*	This work
pEXOM	pEX100Tlink containing 5′–3′ flanking sequence of *oprM*	This work
pEXOMGm	pEX100Tlink containing 5′–3′ flanking sequence of *oprM*::Gm*lox*	This work

[a] Nal, nalidixic acid; Kan, kanamycin; Gm, gentamicin; Ap, ampicillin; MCS, multiple-cloning site; Tc, tetracycline.

or *ampC* mutants were constructed using the *Cre-lox* system for gene deletion and antibiotic resistance marker recycling following previously described protocols (20, 26). Briefly, upstream and downstream PCR products (Table 2) of each gene were digested with either BamHI or EcoRI and HindIII and cloned by three-way ligation into pEX100Tlink with a deletion with respect to the HindIII site and opened by EcoRI and BamHI. The resulting plasmids were transformed into *Escherichia coli* strain XL_1Blue, and transformants were selected on ampicillin-LB agar plates (30 μg/ml). The *lox*-flanked gentamicin resistance cassette (*aac1*) obtained by HindIII restriction of plasmid pUCGm*lox* was cloned into the single site for this enzyme formed by the ligation of the two flanking fragments. The resulting plasmids were again transformed into *E. coli* strain XL_1Blue, and transformants were selected on ampicillin (30 μg/ml)-5 gentamicin (μg/ml)-LB agar plates. Plasmids were then transformed into the *E. coli* S17-1 helper strain. Knockout mutants were generated by conjugation followed by selection of double recombinants by the use of sucrose (5%)-cefotaxime (1 μg/ml)-gentamicin (30 μg/ml)-LB agar plates. Double recombinants were checked first by screening for susceptibility to carbenicillin (200 μg/ml) and afterwards by PCR amplification and sequencing. For the recycling of the gentamicin resistance cassettes, plasmid pCM157 was electroporated into the different mutants. Transformants were selected in tetracycline (250 μg/ml)-LB agar plates. One transformant for each mutant was grown overnight in tetracycline (250 μg/ml)-LB broth in order to allow expression of the *cre* recombinase. Plasmid pCM157 was then cured from the strains by successive passages on LB broth. Selected colonies were then screened for susceptibility to tetracycline (250 μg/ml) and gentamicin (30 μg/ml) and checked by PCR amplification and DNA sequencing. To asses the effect on growth rates of the mutants generated, the doubling times of cells growing exponentially in LB broth at 37°C and 180 rpm were determined by plating serial 10-fold dilutions on LB agar at 1-h intervals as previously described (21). Five independent experiments were performed for each of the mutants, and mean values (± standard deviations [SD]) were determined.

Cloning of *nfxB* and complementation studies. For cloning *nfxB*, the PAO1 wild-type gene was PCR amplified using primers nBF1BHI and nBR2ERI (Table 2). The resulting PCR product was digested with BamHI and EcoRI and ligated to plasmid pUCP24, digested with the same enzymes, to obtain plasmid pUCPNB, which was transformed into *E. coli* strain XL1-Blue. Transformants were selected on gentamicin (5 μg/ml)-MacConkey agar plates. The cloned DNA fragment was fully sequenced to confirm the absence of mutations generated during PCR amplification. Plasmids pUCPNB and pUCP24 (control) were then electroporated into PAO1 or the different *nfxB* mutants. Transformants were selected on gentamicin (30 μg/ml)-LB agar plates.

Susceptibility testing. MICs of the antipseudomonal agents ceftazidime, cefepime, cefotaxime, piperacillin-tazobactam, aztreonam, imipenem, meropenem, ciprofloxacin, and tobramycin were determined using Mueller-Hinton (MH) agar plates and Etest strips in duplicate experiments.

TABLE 2. Primers used in this work

Primer	Sequence (5′–3′)[a]	PCR product size (bp)	Use	Reference or source
ACrnaF	GGGCTGGCCTCGAAAGAGGAC	246	Quantification of *ampC* mRNA	14
ACrnaR	GCACCGAGTCGGGGAACTGCA			
MexB-U	CAAGGGCGTCGGTGACTTCCAG	273	Quantification of *mexB* mRNA	24
MexB-L	ACCTGGGAACCGTCGGGATTGA			
MexD-U	GGAGTTCGGCCAGGTAGTGCTG	236	Quantification of *mexD* mRNA	24
MexD-L	ACTGCATGTCCTCGGGGAAGAA			
MexF-U	CGCCTGGTCACCGAGGAAGAGT	254	Quantification of *mexF* mRNA	24
MexF-L	TAGTCCATGGCTTGCGGGAAGC			
MexY-Fa	TGGAAGTGCAGAACCGCCTG	270	Quantification of *mexY* mRNA	24
MexY-Ra	AGGTCAGCTTGGCCGGGTC			
RpsL-1	GCTGCAAAACTGCCCGCAACG	250	Quantification of *rpsL* mRNA	24
RpsL-2	ACCCGAGGTGTCCAGCGAACC			
OprM-F3	CACTACCGCCTGGGAACTC	259	Quantification of *oprM* mRNA	This work
OprM-R3	GGTCGAGCGCGGAGGCG			
nBF1BHI	TCGGATCCGCACCTCGGCGACCCGC	523	NfxB inactivation	23
nBR1HDIII	TCAAGCTTCGAGCATCTGCACCAGGTTG			
nBF2HDIII	TCAAGCTTGCCTTCTTCCTGCGCGGAC	434		
nBR2ERI	CGGAATTCCTGGGGGAGGTGTG			
DACB-F-ERI	TCGAATTCCGACCATTCGGCGATATGAC	571	DacB inactivation	20
DACB-I-R-HD3	TCAAGCTTGTCGCGCATCAGCAGCCAG			
DACB-I-F-HD3	TCAAGCTTGCCAGGGCAGCGTACCGC	693		
DACB-R-BHI	TCGGATCCCGCGTAATCCGAAGATCCATC			
AmpC-F-ERI	TCGAATTCGCGCGCAGGGCGTTCAG	415	AmpC inactivation	21
AmpC-I-R-HDIII	TCAAGCTTCGTCCTCTTACGAGGCCAG			
AmpC-I-F-HDIII	TCAAGCTTCAGGGCAGCCGCTTCGAC	432		
AmpC-R-BHI	TCGGATCCCAGGTTGGCATCGACGAAG			
mxDF1BHI	TCGGATCCATCAAGCGGCCGAACTTCG	446	MexD inactivation	23
mxDR1HDIII	TCAAGCTTGGTGTCGCTGCGCTGAGC			
mxDF2HDIII	TCAAGCTTCACCACGAGAAGCGCGGCTTC	563		
mxDR2ERI	TCGAATTCAGCAGCGCTTCGCGGCCG			
mxRF1 ERI	TCGAATTCAGCAGGGCCGGAACCAGTA	453	MexR inactivation	This work
mxRR1 HD3	TCAAGCTTCAATACATGGACGTC			
mxRF2 HD3	TCAAGCTTGCGTGCATGACGAGTTGTTTG	558		
mxRR2 BHI	TCGGATCCAGAAGAACCCGTCGGCCGA			
OMF1ERI	TCGAATTCGATCGGTACCGGCGTGATC	471	OprM inactivation	This work
OMR1HDIII	TCAAGCTTACCGTCCACGCCGATCCG			
OMF2HDIII	TCAAGCTTCTTCCCGAGCATCAGCCT	522		
OMR2BHI	TCGGATCCAAGCCTGGGGATCTTCCTTC			

[a] Sites for restriction endonucleases are underlined.

Analysis of whole-genome gene expression. Strains were grown in 10 ml of LB broth at 37°C and 180 rpm to the late log phase (optical density at 600 nm [OD_{600}] of 1). The cells were collected by centrifugation, and total RNA was isolated using an RNeasy minikit (Qiagen). RNA was dissolved in water and treated with 2 U of Turbo DNase (Ambion) for 30 min at 37°C to remove contaminating DNA. The reaction was stopped by the addition of 5 μl of DNase inactivation reagent. Total RNA (10 μg) was checked by the use of an agarose gel prior to cDNA synthesis. cDNA synthesis, fragmentation, labeling, and hybridization were performed according to the Affymetrix GeneChip *P. aeruginosa* genome array expression analysis protocol. Three independent experiments were performed for each strain. Expression analysis was performed as previously described (33). Only transcripts showing increases or decreases that were higher than 2-fold were considered to represent differential expression results. In all cases, the value representing the posterior probability for differential expression (PPDE) was between 0.999 and 1.

Expression of resistance genes. The levels of expression of *ampC*, *mexB*, *mexD*, *mexY*, *mexF*, and *oprM* were determined by real-time reverse transcription-PCR (RT-PCR) following previously described protocols (14, 24). Total RNA was isolated as described above. A 50-ng sample of purified RNA was then used for one-step reverse transcription and real-time PCR amplification using a QuantiTect SYBR green RT-PCR kit (Qiagen) and a SmartCycler II system (Cepheid). The primers listed in Table 2 were used for amplification of *ampC*, *mexB*, *mexD*, *mexY*, *mexF*, *oprM*, and *rpsL* (used as a reference to normalize the relative amounts of mRNA). In all cases, the mean values of relative mRNA expression obtained in at least three independent duplicate experiments were considered. For *ampC* induction experiments, cultures were incubated in the presence of imipenem (0.015 μg/ml).

Penicillin-binding protein (PBP) assays. Late-log-phase (OD_{600} of 1) LB cultures (500 ml) were collected by centrifugation, washed, and suspended in 50 ml of buffer A (20 mM KH_2PO_4–140 mM NaCl [pH 7.5]). Cells were then sonicated and centrifuged at 12,000 × *g* for 10 min. Membranes containing the PBPs were isolated through two steps of ultracentrifugation at 150,000 × *g* for 1 h at 4°C and suspension in buffer A. PBPs were then labeled with a 25 μM concentration of Bocillin FL fluorescent penicillin (36), separated through the use of sodium dodecyl sulfate-polyacrylamide gel electrophoresis (SDS-PAGE), and visualized using a Bio-Rad FX Pro molecular imager.

OMP analysis. A protocol adapted from those previously described (5) was followed. Briefly, late-log-phase (OD_{600} of 1) LB cultures (200 ml) were collected by centrifugation, washed, and suspended in 5 ml of buffer (10 mM Tris-Mg [pH 7.3]). Cells were then sonicated and centrifuged at 7,000 × *g* for 15 min. Membranes were isolated through ultracentrifugation at 100,000 × *g* for 1 h at 4°C. Pellets were suspended in 10 ml of buffer (1% sarcosyl, 25 mM Tris-HCl [pH 8]) and incubated for 30 min at room temperature. Outer membrane proteins (OMPs) were collected afterward through ultracentrifugation at 70,000 × *g* for 40 min, suspended in the same buffer, and ultracentrifuged again. OMPs were then suspended in water, separated using SDS-PAGE (11% acrylamide–0.2% bisacrylamide–0.2% SDS–0.375 M Tris [pH 8.8]), and visualized using Coomassie staining.

β-Lactamase assays. Specific ß-lactamase activity (quantified as nanomoles of nitrocefin hydrolyzed per minute per milligram of protein) was determined

TABLE 3. Susceptibility profiles of the studied *P. aeruginosa* strains

Strain[a]	MIC (μg/ml)[b]								
	CAZ	FEP	CTX	PTZ	ATM	IMP	MER	CIP	TOB
PAO1 (reference strain)	1.5	1.5	8	2	2	1.5	0.38	0.094	1
PAO1-*nfxB*	0.5	6	3	1.5	0.38	0.094	0.125	1.5	0.25
PAO1-*dacB*	24	12	>256	48	12	1.5	0.5	0.094	1
PAO1-*nfxB-dacB*	1.5	6	24	3	0.5	0.125	0.19	1.5	0.25
PAO1-*mexD*	1.5	1.5	8	2	2	1.5	0.38	0.094	1
PAO1-*nfxB-mexD*	1	1.5	8	1.5	2	1.5	0.38	0.094	1
PAO1-*nfxB-dacB-mexD*	24	12	>256	48	12	1.5	0.5	0.094	1
PAO1-*ampC*	1	1.5	6	1.5	1.5	0.19	0.19	0.094	1
PAO1-*nfxB-ampC*	0.75	6	3	1.5	0.38	0.094	0.125	1.5	0.25
PAO1-*oprM*	0.5	0.25	1	0.125	0.125	1	0.094	0.008	0.25
PAO1-*nfxB-oprM*	0.5	6	3	2	0.125	0.094	0.125	1.5	0.19
PAO1-*dacB-oprM*	24	12	>256	24	8	1.5	0.25	0.008	0.25
PAO1-*nxfB-dacB-oprM*	1.5	6	24	2	0.5	0.125	0.19	1.5	0.19
JW (wild-type clinical isolate)	1.5	3	16	4	4	1.5	0.25	0.125	1
JW-*nfxB*	1	32	8	3	1.5	0.38	0.19	1.5	0.38
GPP (wild-type clinical isolate)	1	2	12	3	2	1	0.125	0.125	1
GPP-*nfxB*	0.75	8	4	1.5	0.5	0.25	0.125	1.5	0.25

[a] PAO1-*nfxB* (pUCPNB) and PAO1-*nfxB-dacB* (pUCPNB) showed the same MICs as PAO1 and PAO1-*dacB*, respectively.
[b] CAZ, ceftazidime; FEP, cefepime; CTX, cefotaxime; PTZ, piperacillin-tazobactam; ATM, aztreonam; IMP, imipenem; MER, meropenem; CIP, ciprofloxacin; TOB, tobramycin.

spectrophotometrically, following established procedures (13), on culture supernatants, crude sonic extracts, and periplasmic fractions prepared as described elsewhere (10). Activities were determined at the early log phase (OD_{600} of 0.2), late log phase (OD_{600} of 1), and stationary phase (18 h of incubation). For normalizing total cell numbers in cultures from the different strains, CFU were enumerated by plating serial dilutions in LB agar. For AmpC induction experiments, cultures were incubated in the presence of imipenem (0.015 μg/ml). Mean values (± SD) of β-lactamase activity obtained from at least 3 independent experiments were considered in all cases.

Antimicrobial activity in biofilm growth. Biofilms were formed following previously described protocols (23). Briefly, biofilms were grown by incubating peg lids (Nunc, Denmark) (at 24 h and 37°C under static conditions) in microtiter plates containing MH broth (approximately 2×10^8 cells/ml). Then, biofilms on peg lids were incubated for 24 h in MH broth supplemented with several concentrations of the tested antibiotics or left unsupplemented. Afterwards, biofilms were rinsed and transferred to MH broth by centrifugation (20 min, 1,000 rpm, 4°C). Serial 1/10 dilutions were then plated in MH agar to determine the number of viable cells. All experiments were performed in triplicate.

RESULTS

Antibiotic (hyper)susceptibility profile of *nfxB* mutants and reversion of resistance driven by AmpC hyperproduction. As expected from reports of previous work (8), MexCD-OprJ overexpression in PAO1, driven by *nfxB* mutation, significantly increased the MICs of ciprofloxacin (16-fold) and cefepime (4-fold), which are known to be good substrates for the pump. On the other hand, it produced a significant decrease in the MICs of all other antipseudomonal agents, with the imipenem (16-fold) and tobramycin (4-fold) results being particularly noteworthy, but also of all other β-lactams tested (Table 3). Complementation with the wild-type *nfxB* gene, from the pUCPNB plasmid, fully restored the wild-type PAO1 susceptibility profile. The inactivation of *nfxB* in two genetically unrelated clinical strains yielded very similar susceptibility profiles, demonstrating that the observed phenotype was not specific to the PAO1 background (Table 3). Moreover, the inactivation of *nfxB* nearly reversed the resistance profile (cephalosporins, penicillins, and monobactams) of the AmpC-hyperproducer *dacB* (PBP4) mutant of PAO1 (Table 3). For example, the MICs of ceftazidime decreased from 24 μg/ml for the *dacB* mutant to 1.5 μg/ml (wild-type level) for the *nfxB-dacB* double mutant (Table 3). Complementation with the wild-type *nfxB* gene fully restored the parental *dacB* mutant susceptibility profile.

The inactivation of *mexD* (efflux pump-encoding gene) in the *nfxB* mutant fully restored wild-type (PAO1) susceptibility, and the inactivation of *mexD* in the *nfxB-dacB* mutant fully restored the *dacB* phenotype (Table 3). Therefore, these findings indicate that the observed phenotypes relate directly to the overexpression of the efflux pump and not to the inactivation of its NfxB regulator. Real-time RT-PCR experiments showed that expression of *ampC*, *mexB*, *mexY*, *mexF*, and *oprM* was not significantly modified in the *nfxB* mutant compared to expression of wild-type PAO1. Moreover, while global transcriptome analysis revealed 34 genes (24 upregulated and 10 downregulated) with modified expression in the *nfxB* mutant, only those genes belonging to the *mexC-mexD-oprJ* operon had an obvious link to antibiotic susceptibility (Table 4). Therefore, these findings support the data presented above indicating that transcriptional regulation is not involved in the described NfxB phenotypes. Nevertheless, the effects on cell physiology or fitness of the modified gene expression patterns, including several involved in nitric oxide and iron or copper metabolism and quorum sensing, still need to be elucidated. Indeed, NfxB mutation also resulted in overall fitness reduction, as evidenced by the increased doubling times of growth of the *nfxB* mutant (42.7 ± 8.8) compared to wild-type PAO1 (26.9 ± 6.8), although, again, the results depended directly on overexpression of the efflux pump, since the inactivation of *mexD* in the *nfxB* mutant nearly compensated for the growth defect (doubling time of the *nfxB-mexD* mutant, 30.8 ± 7.1).

Role of impairment of intrinsic efflux in NfxB phenotypes. MexAB-OprM and MexXY-OprM efflux pumps play a central role in *P. aeruginosa* intrinsic resistance. Thus, hypersusceptibility of the *nfxB* mutant could well be driven by the impair-

TABLE 4. Gene loci showing modified expression (>2-fold change) in the *nfxB* mutant compared to the parental wild-type PAO1 strain as determined using Affymetrix GenChips

Gene locus	Product	Fold expression change
PA0524-norB	Nitric oxide reductase subunit B	11.85
PA0523-norC	Nitric oxide reductase subunit C	11.45
PA4599-mexC	Resistance-nodulation-cell division (RND) multidrug efflux membrane fusion protein MexC precursor	11.00
PA4598-mexD	Resistance-nodulation-cell division (RND) multidrug efflux transporter MexD	7.29
PA4597-oprJ	Multidrug efflux outer membrane protein OprJ precursor	5.53
PA0525	Probable denitrification NorD protein	3.99
PA3392-nosZ	Nitrous oxide reductase precursor	3.12
PA4386-groES	GroES protein	3.09
PA0518-nirM	Cytochrome *c*-551 precursor	2.90
PA0519-nirS	Nitrite reductase precursor	2.89
PA0200	Hypothetical protein	2.86
PA0918	Cytochrome *b*-561	2.71
PA4919-pncB1	Nicotinate phosphoribosyltransferase	2.55
PA0517-nirC	Probable *c*-type cytochrome precursor	2.46
PA1432-lasI	Autoinducer synthesis LasI protein	2.38
PA4385-groEL	GroEL protein	2.28
PA4687-hitA	Ferric iron-binding periplasmic HitA protein	2.25
PA3813-iscU	Probable iron-binding IscU protein	2.25
PA0516-nirF	Heme d1 biosynthesis NirF protein	2.16
PA4920-nadE	NH3-dependent NAD synthetase	2.14
PA4918	Hypothetical protein	2.06
PA0024-hemF	Coproporphyrinogen III oxidase, aerobic	2.04
PA5015-aceE	Pyruvate dehydrogenase	2.01
PA1431-rsaL	Regulatory RsaL protein	2.01
PA1555	Probable cytochrome *c*	−2.88
PA1557	Probable cytochrome oxidase (cbb3-type) subunit	−2.85
PA3361-lecB	Fucose-binding lectin PA-IIL	−2.79
PA1556	Probable cytochrome *c* oxidase subunit	−2.71
PA0122	Conserved hypothetical protein	−2.33
PA4133	Cytochrome *c* oxidase (cbb3-type) subunit	−2.33
PA3790-oprC	Putative copper transport outer membrane porin OprC precursor	−2.21
PA4217-phzS	Flavin-containing monooxygenase	−2.20
PA1658	Conserved hypothetical protein	−2.11
PA3205	Hypothetical protein	−2.03

ment of these efflux pumps (8, 12). Indeed, despite the fact that transcription of *oprM* was not modified, in contrast to earlier observations (8), the outer membrane protein (OMP) profiles of the *nfxB* mutants confirmed the previously noted (8) reduced expression of OprM (Fig. 1, lane 1 versus lane 2). More informatively, susceptibility data clearly indicated that OprM was impaired (i.e., did not significantly contribute to resistance) in the *nfxB* mutant (Table 3). While the inactivation of *oprM* in PAO1 produced a remarkable decrease in the MICs of all antibiotics tested (except for imipenem), its inactivation in the *nfxB* (or *nfxB-dacB*) mutant did not have a significant effect on MICs, thus showing that OprM activity was already impaired in the *nfxB* mutants. Indeed, impairment of OprM in the *nfxB* mutant clearly explained the hypersusceptibility to tobramycin (substrate of MexXY-OprM) and to ceftazidime, cefotaxime, piperacillin-tazobactam, aztreonam, and meropenem (substrates of MexAB-OprM), results that are consistent with previous observations (8, 12). On the other hand, it did not explain the imipenem hypersusceptibility, since *oprM* inactivation in PAO1 had a minimal (less than one 2-fold dilution) effect on the MIC of this antibiotic, which is consistent with previous studies showing that imipenem is not significantly extruded by any of these two pumps. Moreover, the efflux pumps were not involved in the reversion of PBP4-driven resistance in the *nfxB-dacB* mutant, since the inactivation of *oprM* in the *dacB* mutant did not reverse its resistance profile at all (Table 3). As shown in Fig. 1, OMP analysis also revealed that expression of the OprD carbapenem porin in the *nfxB* mutant was not significantly modified. Moreover, the PBP expression profile of the *nfxB* mutant was nearly identical to that of wild-type PAO1 (Fig. 2). These findings indicated that neither OprD nor PBPs are involved in the phenotype.

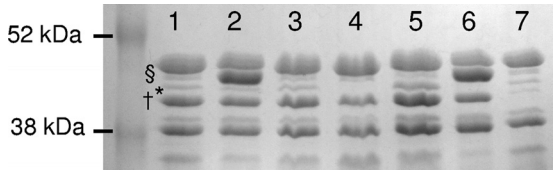

FIG. 1. OMP profiles of wild-type PAO1 and different mutant derivatives. Lane 1, wild-type PAO1 (wild-type profile); lane 2, *nfxB* mutant (overexpression of OprJ, reduced expression of OprM); lane 3, *nfxB-mexD* mutant (wild-type profile); lane 4, *oprM* mutant (no expression of OprM); lane 5, *mexR* mutant (overexpression of OprM); lane 6, *nfxB-oprM* mutant (overexpression of OprJ, no expression of OprM); lane 7, *oprD* mutant (no expression of OprD). Bands corresponding to OprD (†), OprM (*), and OprJ (§) are indicated.

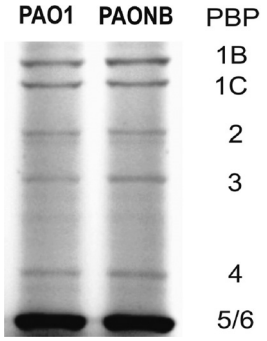

FIG. 2. PBP expression profiles of wild-type strain PAO1 and its *nfxB* knockout mutant (PAONB).

Altered β-lactamase physiology in *nfxB* mutants. Data concerning the possible involvement of AmpC in the *nfxB* phenotype have remained elusive and controversial for years (16, 19, 34). As described above, the *nfxB* mutant showed no modified *ampC* expression. Moreover, as shown in Table 5, *ampC* in the *nfxB* mutant was still highly inducible in the presence of subinhibitory concentrations of imipenem and still highly overexpressed in the *nfxB-dacB* double mutant. Similarly, crude (total) β-lactamase activity (basal or imipenem induced) was not significantly modified in the corresponding *nfxB* mutants (Table 5). These results should therefore support those of previous works concluding that AmpC is not involved (34), but a deeper analysis of AmpC physiology revealed that this is not actually the case. Indeed, a dramatic decrease in constitutive and induced periplasmic AmpC activity was noted in the *nfxB* mutants compared to the results seen with the respective parent strains (Table 5). Moreover, inducible (Fig. 3A) and constitutively overexpressed (Fig. 3B) AmpC activity in the periplasm was significantly impaired in the exponential-growth phase but not in the stationary phase. Obviously, the impairment of inducible and constitutively overexpressed AmpC activity in the location (periplasm) and growth phase (exponential growth) where it is expected to protect the drug targets (essential PBPs) should certainly explain the imipenem hypersusceptibility and reversion of PBP4-driven resistance. Accordingly, the susceptibility data of Table 3 with respect to the *ampC* mutants totally support the finding of impaired AmpC activity in the *nfxB* mutant. As would be expected, the inactivation of *ampC* in PAO1 dramatically reduced imipenem MICs (imipenem is a very strong AmpC inducer, despite its relative stability with respect to hydrolysis) but it had no major effect on susceptibility to other antipseudomonal β-lactams (very weak AmpC inducers, despite being efficiently hydrolyzed). On the other hand, the inactivation of a*mpC* in the *nfxB* mutant did not further decrease the imipenem MICs, showing that AmpC activity was already impaired in the single *nfxB* mutant.

Additional analysis revealed that the imipenem-induced *nfxB* mutant and the *nfxB-dacB* mutant showed significantly higher AmpC activity on culture supernatants than their respective parent strains (Table 5, Fig. 3). This result further suggested that impairment of periplasmic AmpC activity in PAO1 does not result from a defective AmpC exportation from the cytoplasm to the periplasm but more likely from an

TABLE 5. Basal and induced *ampC* expression and β-lactamase activity of crude, periplasmic, and culture supernatants for the studied mutants

Strain	*ampC* mRNA[a]		β-Lactamase activity[b]					
			Crude		Periplasmic		Supernatant	
	Basal	Induced	Basal	Induced[c]	Basal	Induced[c]	Basal	Induced[c]
PAO1	1	19 ± 5.5	164 ± 36 (16 ± 5.9)	4,714 ± 1,473 (353 ± 247)	34 ± 5.1 (9.5 ± 2.6)	590 ± 231 (210 ± 76)	ND[d]	228 ± 135 (296 ± 176)
PAO1-*nfxB*	1.2 ± 0.2	27 ± 6.5	148 ± 40 (13 ± 1.8)	7,526 ± 1,269 (625 ± 391)	13 ± 4.2 (4.5 ± 1.7)	102 ± 25 (33 ± 17)	ND	975 ± 345 (1,365 ± 483)
PAO1-*nfxB-mexD*	0.8 ± 0.1	13 ± 2.0	227 ± 33 (28 ± 7.5)	4,189 ± 346 (451 ± 279)	37 ± 8.6 (13 ± 7.3)	428 ± 85 (150 ± 49)	ND	326 ± 243 (359 ± 267)
PAO1-*dacB*	49 ± 9.5	72 ± 26	8,949 ± 2,911 (875 ± 254)	13,278 ± 3,031 (1,006 ± 477)	2,087 ± 495 (532 ± 114)	3,525 ± 442 (745 ± 364)	213 ± 77 (256 ± 92)	1,124 ± 576 (1,574 ± 806)
PAO1-*nfxB-dacB*	25 ± 5.4	58 ± 6.3	6,924 ± 2,635 (878 ± 470)	15,746 ± 5,371 (1,709 ± 437)	131 ± 20 (50 ± 19)	361 ± 67 (116 ± 68)	1,210 ± 234 (1,573 ± 304)	1,850 ± 817 (2,590 ± 1,138)

[a] Results represent relative *ampC* mRNA levels compared to the levels seen with strain PAO1 under basal (noninduced) conditions.

[b] Results represent picomoles of nitrocefin hydrolyzed per minute per milligram of protein (crude and periplasmic β-lactamase activity) or per milliliter (supernatant β-lactamase activity). β-Lactamase activity levels (expressed in picomoles of nitrocefin hydrolyzed per min) per 10^9 CFU are shown in parentheses.

[c] Induction experiments were carried out in the presence of imipenem at 0.015 mg/liter, corresponding to the lowest concentration of the antibiotic not compromising the growth rate of the *nfxB* mutant (ca. 0.25× MIC). The corresponding data for strain PAO1, determined using an equivalent (with respect to the MIC) concentration of imipenem (0.25 mg/liter [0.25× MIC]), were 60 for ampC mRNA, 7,152 for crude β-lactamase activity, 750 for periplasmic β-lactamase activity, and 425 for supernatant β-lactamase activity.

[d] ND, β-lactamase activity was too low for accurate detection.

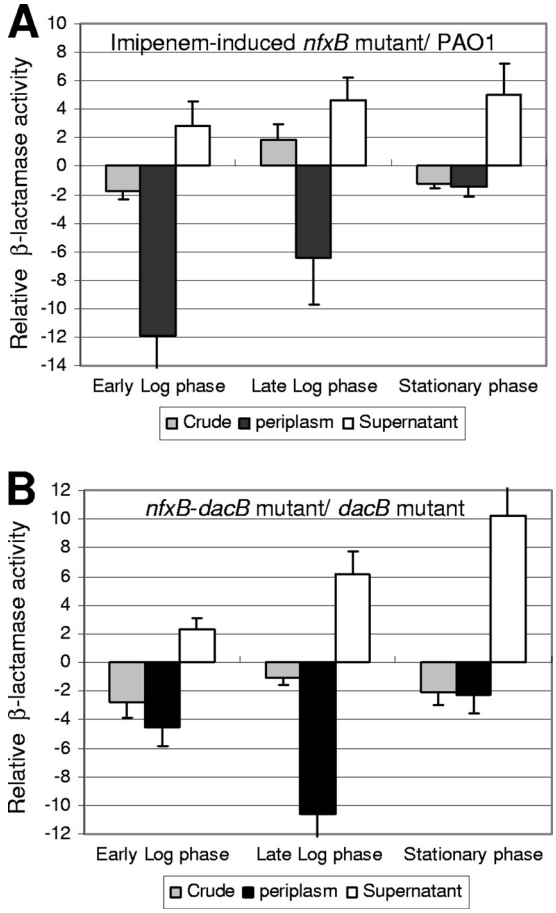

FIG. 3. (A) Relative imipenem-induced crude, periplasmic, and culture supernatant AmpC activity levels of the *nfxB* mutant compared to parent wild-type PAO1 levels at different growth phases. (B) Relative basal (constitutive) crude, periplasmic, and culture supernatant AmpC activity levels of the *nfxB-dacB* mutant compared to parent *dacB* mutant levels at different growth phases.

altered outer membrane physiology produced by MexCD-OprJ overexpression, leading to AmpC leakage out of the cell. Moreover, as shown in Fig. 4, the increased leakage of AmpC resulting from *nfxB* inactivation was also observed for the clinical isolates JW and GPP, demonstrating the this phenomenon is not specific to PAO1.

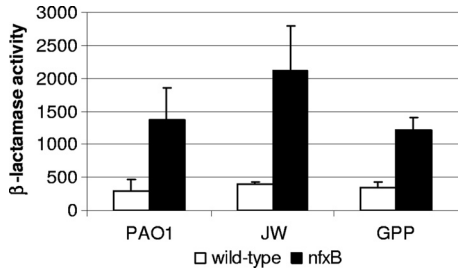

FIG. 4. Imipenem-induced AmpC activity (in picomoles of nitrocefin hydrolyzed per minute) per milliliter of supernatant from late-log-phase cultures (OD_{600} of 1 [adjusted to 10^9 CFU/ml]) of wild-type strains PAO1 (reference strain), JW, and GPP (clinical isolates) compared to that of their respective *nfxB* mutants.

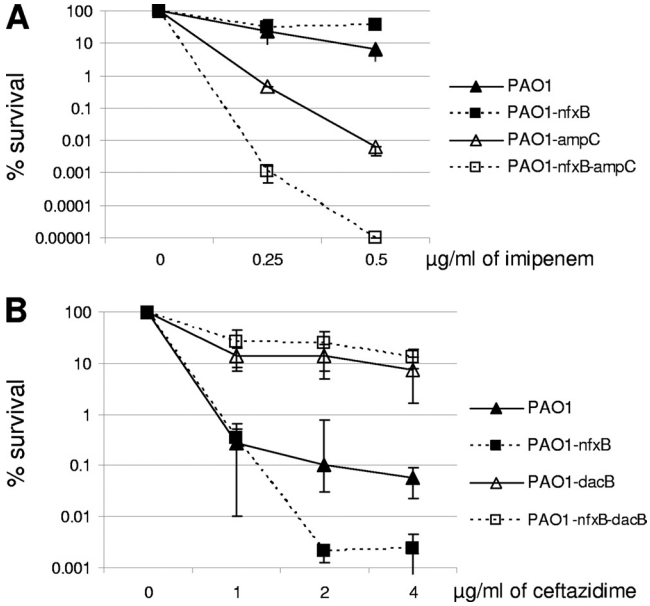

FIG. 5. (A) Activity of imipenem (strong AmpC inducer but weakly hydrolyzed) against biofilms formed by wild-type strain PAO1 and its *nfxB*, *ampC*, and *nfxB-ampC* knockout mutants. (B) Activity of ceftazidime (very weak AmpC inducer but readily hydrolyzed) against biofilms formed by wild-type strain PAO1 and its *nfxB*, *dacB*, and *nfxB-dacB* knockout mutants. The results shown represent mean (± SD) relative survival percentages (corresponding to viable cells in treated versus nontreated biofilms) after 24 h of incubation in the presence of different concentrations of the antibiotics.

Modified β-lactamase physiology in *nfxB* mutants is protective in biofilm growth. It seems obvious that failure to concentrate AmpC activity in the periplasm should dramatically limit the capacity of this enzyme to protect the PBP targets of β-lactam antibiotics at the individual cell level, but perhaps the expected outcome for cells growing as biofilm communities is less obvious, as they are surrounded by a thick extracellular matrix that could trap the leaked β-lactamase. Indeed, the results presented in Fig. 5 indicate that AmpC secreted by *nfxB* mutants is protective in biofilm growth. First, Fig. 5A shows that inducible AmpC expression is protective in the *nfxB* mutant since (i) imipenem hypersusceptibility was not observed and (ii) inactivation of *ampC* in the *nfxB* mutant markedly increased imipenem susceptibility. Second, Fig. 5B shows that constitutively overexpressed AmpC is also protective, since (i) ceftazidime resistance driven by AmpC overexpression (*dacB* inactivation) is not reversed through the inactivation of *nfxB* and (ii) the inactivation of *dacB* in the *nfxB* mutant sharply increased ceftazidime resistance. Thus, these results clearly indicate that resistance driven by inducible and constitutively overexpressed AmpC is not impaired when the *nfxB* mutants grow as biofilm communities, sharply contrasting with the results shown above for planktonically growing cells.

DISCUSSION

Deciphering the complex interactions between resistance pathways is critical for guiding future strategies for the management of *P. aeruginosa* infections, through the identification

of new targets or regimens (such as particular combinations of antimicrobial agents) to overcome resistance mechanisms. In this sense our results were encouraging, showing that these interactions among resistance pathways are not always synergistic. Indeed, we confirmed previous evidence (8, 12, 19) indicating that overexpression of the MexCD-OprJ efflux pump (through the mutational inactivation of its negative regulator NfxB) may impair the backbone of related *P. aeruginosa* intrinsic resistance mechanisms, which include the major constitutive (MexAB-OprM) and inducible (MexXY-OprM) efflux pumps, together with the inducible chromosomal cephalosporinase AmpC. Moreover, we further demonstrated that it reversed the most relevant mechanism leading to acquired β-lactam resistance in *P. aeruginosa*, mutation-driven constitutive overexpression of AmpC. Our results indicated that impairment of intrinsic and acquired resistance occurs at the posttranscriptional level and depends on overexpression of the MexCD-OprJ efflux pump itself and not on the mutation of its negative regulator NfxB. While impairment of intrinsic pumps (MexAB-OprM and MexXY-OprM) upon MexCD-OprJ overexpression could well result from a compensatory balance of efflux machinery in the cell envelope, the explanation accounting for impairment of inducible and constitutive AmpC activity seemed less obvious. Indeed, neither *ampC* transcription nor crude (total) β-lactamase activity (basal or imipenem induced) was significantly modified in the *nfxB* mutants. Therefore, these results should have supported those of previous works concluding that AmpC is not involved (34), but a deeper analysis of AmpC physiology revealed that this was not actually the case. Indeed, a dramatic decrease in basal and induced periplasmic AmpC activity was noted in the *nfxB* mutants compared to the results seen with the respective parent strains. Obviously, the impairment of basal and induced AmpC activity in the location where it is expected to protect the drug targets (PBPs) should certainly explain the reversion of AmpC-driven resistance.

Additional analysis revealed that the imipenem-induced *nfxB* mutant and the *nfxB-dacB* mutant showed increased AmpC activity in culture supernatants. This result further indicates that impairment of periplasmic AmpC activity does not result from defective AmpC exportation to the periplasm from the cytoplasm but likely results from altered outer membrane physiology produced by MexCD-OprJ overexpression, leading to AmpC leakage from the cell. This claim is consistent with recent data showing that MexCD-OprJ overexpression produces major changes in membrane physiology, leading to a significantly modified exoproteome (30), and with the reduced growth rates documented for the *nfxB* mutant. Indeed, MexCD-OprJ expression has been shown to be inducible by a wide variety of membrane-damaging agents as part of the AlgU-controlled envelope stress response (6). From the therapeutic perspective, these results could delineate future strategies to be explored for combating antibiotic resistance in *P. aeruginosa* acute nosocomial infections, combining MexCD-OprJ inducers with classical antipseudomonal agents such as β-lactams or aminoglycosides.

The major drawback for the potential exploitation of the described antagonistic interaction between resistance mechanisms, as has occurred for many of our therapeutic approaches in the past, came from the differential bacterial physiology characteristics that occur in biofilm growth, a hallmark of chronic respiratory infections by *P. aeruginosa*. While it seemed obvious that failure to concentrate AmpC activity in the periplasm should dramatically limit the capacity of this enzyme to protect the targets (PBPs) of β-lactam antibiotics at the individual cell level, the expected outcome for cells growing as biofilm communities was less obvious, as they are surrounded by a thick extracellular matrix. Indeed, our results confirmed this fear, indicating that AmpC produced by *nfxB* mutants is fully protective in biofilm growth. Thus, our research strongly suggests that the release of AmpC into the matrix appears to protect biofilm communities against harmful β-lactams and is consistent with previous studies showing that extracellular AmpC plays a major role in biofilm resistance (1, 2). Unfortunately, this is bad news for the treatment of biofilm-driven infections that are indeed strongly linked to MexCD-OprJ overexpression, as evidenced by its (specific) high prevalence in chronic lung infection in cases of cystic fibrosis (11), its induction (7) and/or selection (23) during biofilm growth, and its involvement in early adaptation to the chronic setting (27), perhaps through mitigating acute virulence effectors (such as the type III secretion system) and promoting biofilm growth (15, 28). Finally, in addition to the therapeutic implications, our findings have important diagnostic consequences, since they denote that AmpC-driven resistance cannot be detected by conventional susceptibility tests performed in the frequent *nfxB* background of chronic infections, adding further evidence to support the studies showing a lack of correlation between susceptibility results and clinical responses (29).

ACKNOWLEDGMENTS

We are grateful to Jonathan McFarland for his help with correction of the English.

This work was supported by Ministerio de Ciencia e Innovación, Instituto de Salud Carlos III, and cofinanced by the European Development Regional Fund (ERDF; "A way to achieve Europe"), by the Spanish Network for Research in Infectious Diseases (REIPI RD06/0008), and by grant PS09/00033.

REFERENCES

1. **Bagge, N., et al.** 2004. Dynamics and spatial distribution of β-lactamase expression in *Pseudomonas aeruginosa* biofilms. Antimicrob. Agents Chemother. **48:**1168–1174.
2. **Bagge, N., et al.** 2004. *Pseudomonas aeruginosa* biofilms exposed to imipenem exhibit changes in global gene expression and β-lactamase and alginate production. Antimicrob. Agents Chemother. **48:**1175–1187.
3. **Costerton, J. W., P. S. Stewart, and E. P. Greenberg.** 1999. Bacterial biofilms: a common cause of persistent infections. Science **284:**1318–1322.
4. **Fajardo, A., et al.** 2008. The neglected intrinsic resistome of bacterial pathogens. PLoS One **3:**e1619.
5. **Filip, C., G. Fletcher, J. L. Wulf, and C. F. Earhart.** 1973. Solubilization of the cytoplasmic membrane of *Escherichia coli* by the ionic detergent sodium-lauryl sarcosinate. J. Bacteriol. **115:**717–722.
6. **Fraud, S., A. J. Campigotto, Z. Chen, and K. Poole.** 2008. MexCD-OprJ multidrug efflux system of *Pseudomonas aeruginosa*: involvement in chlorhexidine resistance and induction by membrane-damaging agents dependent upon the AlgU stress response sigma factor. Antimicrob. Agents Chemother. **52:**4478–4482.
7. **Gillis, R. J., et al.** 2005. Molecular basis of azithromycin-resistant *Pseudomonas aeruginosa* biofilms. Antimicrob. Agents Chemother. **49:**3858–3867.
8. **Gotoh, N., et al.** 1998. Characterization of the MexC-MexD-OprJ multidrug efflux system in Δ*mexA-mexB-oprM* mutants of *Pseudomonas aeruginosa*. Antimicrob. Agents Chemother. **42:**1938–1943.
9. **Høiby, N., T. Bjamsholt, M. Givskov, S. Molin, and O. Ciofu.** 2010. Antibiotic resistance of bacterial biofilms. Int. J. Antimicrob. Agents **35:**322–332.
10. **Imperi, F., F. Tiburzi, and P. Visca.** 2009. Molecular basis of pyoverdine siderophore recycling in *Pseudomonas aeruginosa*. Proc. Natl. Acad. Sci. U. S. A. **106:**20440–20445.
11. **Jalal, S., O. Ciofu, N. Hoiby, N. Gotoh, and B. Wretlind.** 2000. Molecular

mechanisms of fluoroquinolone resistance in *Pseudomonas aeruginosa* isolates from cystic fibrosis patients. Antimicrob. Agents Chemother. **44:**710–712.

12. **Jeannot, K., et al.** 2008. Resistance and virulence of *Pseudomonas aeruginosa* clinical strains overproducing the MexCD-OprJ efflux pump. Antimicrob. Agents Chemother. **52:**2455–2462.
13. **Juan, C., et al.** 2005. Molecular mechanisms of β-lactam resistance mediated by AmpC hyperproduction in *Pseudomonas aeruginosa* clinical strains. Antimicrob. Agents Chemother. **49:**4733–4738.
14. **Juan, C., B. Moya, J. L. Perez, and A. Oliver.** 2006. Stepwise upregulation of the *Pseudomonas aeruginosa* chromosomal cephalosporinase conferring high level beta-lactam resistance involves three AmpD homologues. Antimicrob. Agents Chemother. **50:**1780–1787.
15. **Linares, J. F., et al.** 2005. Overexpression of the multidrug efflux pumps MexCD-OprJ and MexEF-OprN is associated with a reduction of type III secretion in *Pseudomonas aeruginosa*. J. Bacteriol. **187:**1384–1391.
16. **Lister, P. D., D. J. Wolter, and N. D. Hanson.** 2009. Antibacterial-resistant *Pseudomonas aeruginosa*: clinical impact and complex regulation of chromosomally encoded resistance mechanisms. Clin. Microbiol. Rev. **22:**582–610.
17. **Livermore, D. M.** 2002. Multiple mechanisms of antimicrobial resistance in *Pseudomonas aeruginosa*: our worst nightmare? Clin. Infect. Dis. **34:**634–640.
18. **Lyczak, J. B., C. L. Cannon, and G. B. Pier.** 2002. Lung infection associated with cystic fibrosis. Clin. Microbiol. Rev. **15:**194–222.
19. **Masuda, N., E. Sakagawa, S. Ohya, N. Gotoh, and T. T. Nishino.** 2001. Hypersusceptibility of the *Pseudomonas aeruginosa nfxB* mutant to β-lactams due to reduced expression of the AmpC β-lactamase. Antimicrob. Agents Chemother. **45:**1284–1286.
20. **Moya, B., et al.** 2009. β-lactam resistance response triggered by inactivation of a nonessential penicillin-binding protein. PLoS Pathog. **5:**e1000353.
21. **Moya, B., C. Juan, S. Alberti, J. L. Perez, and A. Oliver.** 2008. Benefit of having multiple *ampD* genes for acquiring β-lactam resistance without losing fitness and virulence in *Pseudomonas aeruginosa*. Antimicrob. Agents Chemother. **52:**3694–3700.
22. **Moya, B., et al.** 2010. Activity of a new cephalosporin, CXA-101 (FR264205), against β-lactam-resistant *Pseudomonas aeruginosa* mutants selected in vitro and after antipseudomonal treatment of intensive care unit patients. Antimicrob. Agents Chemother. **54:**1213–1217.
23. **Mulet, X., et al.** 2009. Azithromycin in *Pseudomonas aeruginosa* biofilms: bactericidal activity and selection of *nfxB* mutants. Antimicrob. Agents Chemother. **53:**1552–1560.
24. **Oh, H., S. Stenhoff, S. Jalal, and B. Wretlind.** 2003. Role of efflux pumps and mutations in genes for topoisomerases II and IV in fluoroquinolone-resistant *Pseudomonas aeruginosa* strains. Microb. Drug Res. **9:**323–328.
25. **Poole, K.** 2004. Efflux mediated multiresistance in Gram-negative bacteria. Clin. Microbiol. Infect. **10:**12–26.
26. **Quénée, L., D. Lamotte, and B. Polack.** 2005. Combined *sacB*-based negative selection and cre-lox antibiotic marker recycling for efficient gene deletion in *Pseudomonas aeruginosa*. Biotechniques **38:**63–67.
27. **Rau, M. H., et al.** 2010. Early adaptive developments of *Pseudomonas aeruginosa* after transition from the life in the environment to persistent colonization in the airways of human cystic fibrosis hosts. Environ. Microbiol. **12:**1643–1648.
28. **Sánchez, P., et al.** 2002. Fitness of *in vitro* selected *Pseudomonas aeruginosa nalB* and *nfxB* multidrug resistant mutants. J. Antimicrob. Chemother. **50:**657–664.
29. **Smith, A. L., S. B. Fiel, N. Mayer-Hamblett, B. Ramsey, and J. L. Burns.** 2003. Susceptibility testing of *Pseudomonas aeruginosa* isolates and clinical response to parenteral antibiotic administration: lack of association in cystic fibrosis. Chest **123:**1495–1502.
30. **Stickland, H. G., P. W. Davenport, K. S. Lilley, J. L. Griffin, and M. Welch.** 2010. Mutation of *nfxB* causes global changes in the physiology and metabolism of *P. aeruginosa*. J. Proteome Res. **9:**2957–2967.
31. **Vincent, J. L.** 2003. Nosocomial infections in adult intensive-care units. Lancet **361:**2068–2077.
32. **West, S. E., H. P. Schweizer, C. Dall, A. K. Sample, and L. J. Runyen-Janecky.** 1994. Construction of improved *Escherichia-Pseudomonas* shuttle vectors derived from pUC18/19 and sequence of the region required for their replication in *Pseudomonas aeruginosa*. Gene **148:**81–86.
33. **Winsor, G. L., et al.** 2005. *Pseudomonas aeruginosa* genome database and PseudoCAP: facilitating community-based, continually updated, genome annotation. Nucleic Acids Res. **33**(database issue)**:**D338–D343.
34. **Wolter, D. J., N. D. Hanson, and P. D. Lister.** 2005. AmpC and OprD are not involved in the mechanism of imipenem hypersusceptibility among *Pseudomonas aeruginosa* isolates overexpressing the *mexCD-oprJ* efflux pump. Antimicrob. Agents Chemother. **49:**4763–4766.
35. **Zamorano, L., B. Moyá, C. Juan, and A. Oliver.** 2010. Differential β-lactam resistance response driven by *ampD* or *dacB* (PBP4) inactivation in genetically diverse *Pseudomonas aeruginosa* clinical strains. J. Antimicrob. Chemother. **65:**1540–1542.
36. **Zhao, G., T. I. Meier, S. D. Kahi, K. R. Gee, and L. C. Blaszczak.** 1999. BOCILLIN FL, a sensitive and commercially available reagent for detection of penicillin-binding proteins. Antimicrob. Agents Chemother. **43:**1124–1128.